ARTICLE

Effects of Hydroxylamine Sulfate and Sodium Nitrite on Microstructure and Friction Behavior of Zinc Phosphating Coating on High Carbon Steel

Yu-dong Xu[a*], San Qi[a], Lei Wang[a], Min Shi[a*], Ning Ding[b], Zhi-cheng Pang[b], Quan Wang[a], Xu-dong Peng[a]

a. School of Materials Science and Engineering, Hefei University of Technology, Hefei 230009, China
b. Bengbu Yucheng New Materials Science & Technology Ltd. Co., Bengbu 233000, China

(Dated: Received on November 28, 2014; Accepted on January 27, 2015)

Hydroxylamine sulfate (HAS) and sodium nitrite are used as the accelerators for zinc phosphate coating on high carbon steel. Phase evolution of phosphate coating was investigated by X-ray diffraction. It is found that the phosphating coatings are mainly composed of hopeite $Zn_3Fe(PO_4)_2{\cdot}4H_2O$ and phosphophyllite $Zn_2Fe(PO_4)_2{\cdot}4H_2O$. The microstructural changes of the phosphate coating, as a function of phosphating time, were evaluated by scanning electron microscopy. Four-ball friction experiments reveal that hydroxylamine sulfate instead of sodium nitrite can effectively reduce the friction coefficient of lubricated phosphating coating. Therefore, it may be expected that HAS will be widely used as a fast and ECO-friendly accelerator in phosphate industry.

Key words: Hydroxylamine sulfate, Accelerator, Phosphate coating, Friction

I. INTRODUCTION

Zinc phosphating is usually employed for the pretreatment prior to painting, mainly increasing corrosion protection and enhancing the adherent properties between phosphating coating and painting. Subsequently, zinc phosphating has been extended to other application areas, such as, cold forming (cold drawing [1], cold forging [2], and cold heading, *etc.*), to improve the sliding friction properties of components in sliding contact. Generally speaking, zinc phosphate coatings exhibit the advantages of low cost, good corrosion resistance, good wear/friction resistance and good lubrication behavior [3−6]. Nowadays, the conventional accelerator agents utilized in phosphating solution and coating mainly include nitrite, chlorate, nitrate, peroxides, *etc.*, which can necessarily result in severe environmental protection issues (for instance, emission of nitrogen oxides and greenhouse gases, wastewater discharge and waste discharge, *etc.*). Consequently, more and more researchers and engineers are devoted to the development of more ECO-friendly phosphating technologies, *e.g.* $NaNO_2$-free phosphating bath [7], zinc phosphating accelerated by hydroxylamine, *etc.*

As an environmental friendly oxidizer accelerator, hydroxylamine sulfate (HAS) has been attempted to replace conventional oxidants owing to its good stability, no emission of harmful nitrogen oxides [8, 9] and no discharge of disgusting wastewater and waste. Nowadays, some researches indicate that hydroxylamine can facilitate the formation of a darker, denser and better alkali-resistant zinc phosphating coating in comparison with sodium nitrite. Furthermore, it has been confirmed that HAS can also facilitate the formation of zinc phosphating crystals even at very low temperature (5 °C). Noticeably, zinc phosphating accelerated by HAS are mainly applied in pretreatment prior to painting [10, 11]. The influence of lubricants has been investigated on the friction behavior of zinc phosphated coatings in terms of physical-chemical interactions between lubricant and phosphate. Farias *et al.* [12] and Kumar *et al.* [13] also presented an in-depth investigation of the influence of process parameters on zinc phosphating of medium carbon steel and found that the phosphate needles in phosphating coatings reduced the wear resistance, making the friction coefficient increase and the hardness of the phosphate layer reduce. Lazzarotto *et al.* [14] investigated the effects of processing bath parameters on the quality and performance of zinc phosphate stearate coatings. In addition, it is also important to note that besides the accelerator, other additives such as niobium and nickel ions [15], calcium ions [16], manganese ions [17], tartaric acid [18], and fluoride ions [19] were used to refine the phosphate coatings and improve the corrosion and adhesion properties. However, till now, no application of HAS-accelerated zinc phosphating in cold drawing of high carbon steel has been reported.

In this work, we make an attempt to investigate the effect of HAS and sodium nitrite on the phase formation and morphological evolution during zinc phosphating

*Authors to whom correspondence should be addressed. E-mail: drxyd123@163.com, mrshimin@126.com, Tel./FAX: +86-551-62901362

processing. In addition, four-ball friction experiments were conducted in order to evaluate the friction behavior of lubricated zinc phosphating coating accelerated by HAS and sodium nitrite.

II. EXPERIMENTS

A. Sample preparation

High carbon steel plates (C: 0.8−0.94, Si: 0.15−0.30, Mn: 0.70−1.0, P: ≤0.04, S: ≤0.05) were utilized as the substrate for zinc phosphating. It is well known that a higher content of carbon in steel will result in a faster hardening effect during cold deformation, which has a seriously adverse effect on the subsequent cold plastic processing (cold drawing, cold heading, *etc.*). Consequently, it is very important to investigate the phosphating behavior and friction behavior of high carbon steel materials which are usually utilized in the wire drawing. In this work, the samples were burnished by sand paper after alkali degreasing, and then washed with deionized water. Then, the ingredients of phosphate solution mainly include phosphoric acid (25.65 g/L), zinc oxide (6.26 g/L), hexahydrate zinc nitrite (43.85 g/L), and accelerator (sodium nitrite or hydroxylamine sulfate).

B. Electrochemical characterization

The schematic of electrochemical experiment device is shown in Fig.1. An "open-circuit potential versus time" method was adopted to measure the changes of surface potential with time. In the experiment the saturated calomel electrodes were used as the reference electrode (+241.5 mV) and samples as working electrode, respectively. In addition, the saturated KCl solution was used as the salt bridge between phosphate solution and saturated calomel electrode. The voltage ranges from −0.6 V to −0.4 V and experiments were conducted at 25 °C.

C. Surface morphology characterization

The surface morphology of the phosphated sample was characterized by scanning electron microscope (JSM-6490LV, Japan Electronics Co., Ltd.) and phase characterization as well as composition analyses of the phosphate coating were conducted by X-ray diffraction (X'Pert Pro, Cu-Kα, PAN alytical B.V.) and EDS device. After saponification treatment, the samples were then dried and used in the following four-ball friction tests.

D. Friction test

Four-ball method was utilized to test the friction properties of lubricated phosphating coating and samples. Figure 2 shows the schematic of four-ball friction device, in which the topmost ball was treated by phosphating, and saponification and the three balls below it are annealed high carbon steel balls without phosphating and saponification. In the friction experiment, the speed and loading force were set as 180 r/min, 100 N, respectively.

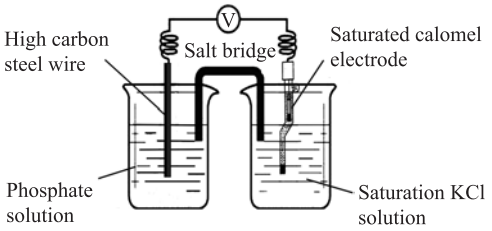

FIG. 1 The schematic of electrochemical test.

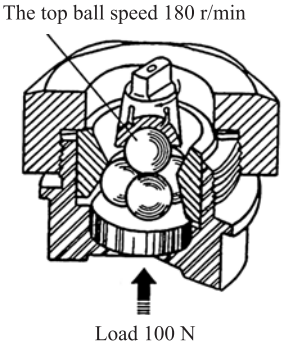

FIG. 2 The schematic of four-ball friction experiment.

TABLE I The optimal conditions for $NaNO_2$ and HAS-accelerated phosphating solutions

	Temperature/°C	Time/min	Concentration/(g/L)
$NaNO_2$	60	9	0.4
HAS	60	3	8

E. Optimization of the phosphating process

Based on the friction experiments, the phosphating parameters including temperature, time and the concentration of accelerators were optimized by utilizing the so-called orthogonal test method (see Table I).

III. RESULTS AND DISCUSSION

A. Electrochemical characterization of the growth process of phosphating coating

The variation of surface potentials with phosphating time at different accelerator concentrations is given in Fig.3. As shown in Fig.3, surface potential-time curve can be divided into three stages whether phosphating

DOI:10.1063/1674-0068/28/cjcp1411201

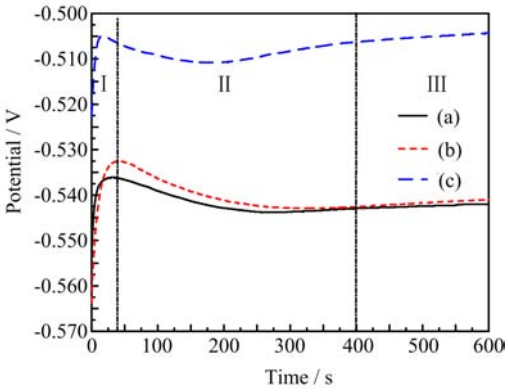

FIG. 3 The dependence of phosphating time on the surface potential at different concentrations of accelerators. (a) 8 g/L hydroxylamine sulfate, (b) basic solution, and (c) 0.4 g/L $NaNO_2$. Surface potential-time curve can be divided into three stages I, II, and III.

liquid contains any accelerators or not. In the first stage I, the dissolution rate of phosphatizing steels is faster than growth rate of phosphating film because a increase of the surface potential results in the loss of electrons of a large number of iron atoms. Afterwards, the surface potential of steels reaches a maximum value when the pH of steel surfaces is in contact with the phosphating liquid increases to a certain value in the stage II phase. During this time, the dissolution reaction rate of steel is lower than the rate of phosphating film formation, therefore, the surface potential begins to decline and corresponding nucleation of phosphate crystal on steel surfaces occurs gradually. In fact, the next stage III can be recognized as a rearrangement and reorientation process of the phosphate crystals. That is, the phosphate crystals starts to grow at a preferred orientation and then the phosphating coating is getting thicker gradually, which unavoidablely prevents the substrate from reacting with the phosphating liquid. At this time, the surface potential of the metal is getting to increase fairly slowly and the thickness of the phospahting coating remains nearly unchanged. As shown in Fig.3(c), the surface potential of the metal decreases after sodium nitrite is added to phosphating solution and the time required for the reaction of the three stages becomes shorter. In contrast, the surface potential of the metal is higher than that of the original solution and phosphating solution when hydroxylamine sulfate is added, but the time required for the reactions is greatly reduced.

B. Surface morphology of phosphating coatings

Figure 4 displays the SEM surface morphologies of phosphate coatings with two kinds of accelerators at different reaction times (Fig.4 (a), (c), (e), (g), and (h) for the samples with sodium nitrite addition and Fig.4 (b), (d), (f), (h), and (j) for those with hydroxylamine sulfate addition). From Fig.4 (a) and (b) it can be found that a small amount of strip and granular phosphate crystals on metal surfaces are formed, and the number of phosphate crystals (Fig.4(b)) is larger than that in Fig.4(a) at 30 s. Next, crystals have covered most of the metal surfaces at 90 s, but exhibit a diverse and different shape: irregularly dendritic in Fig.4(c) and irregular flake in Fig.4(d); At 180 s, crystals have covered all of the metal surfaces and the size of the phosphate crystals gets to increase. Subsequently, the rearrangement and reorientation of the crystals takes place at the time from 180 s to 360 s and the size of phosphate crystalline

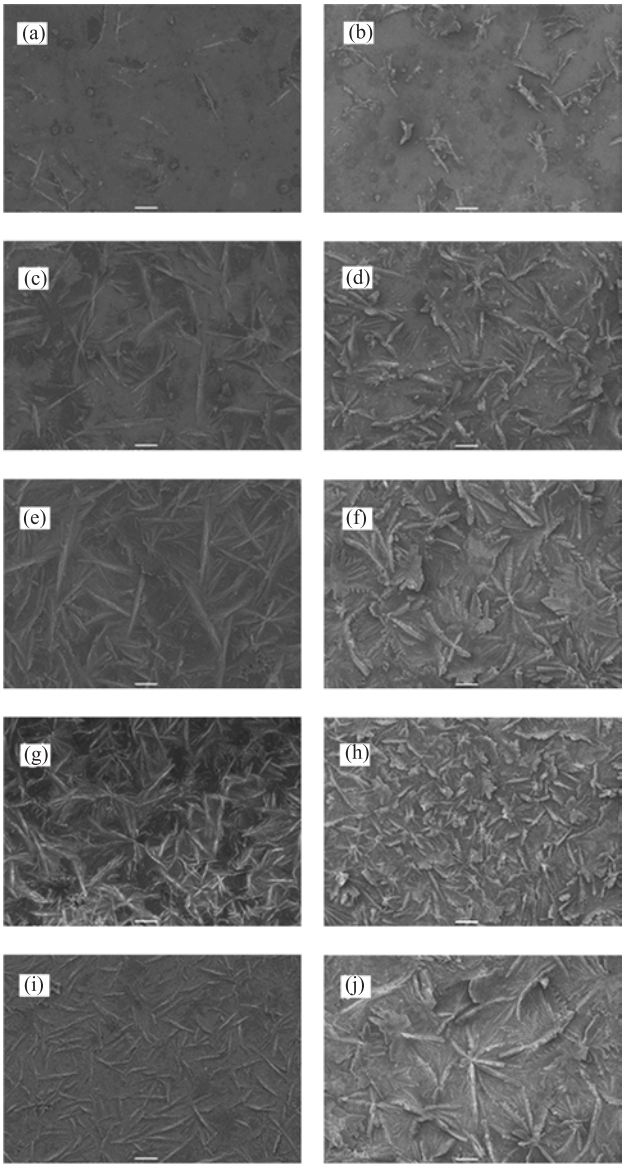

FIG. 4 The SEM images of phosphatizing samples. (a, c, e, g, h) are treated by $NaNO_2$ at 30, 90, 180, 360, and 540 s, respectively. (b, d, f, h, j) are treated by hydroxylamine sulfate at 30, 90, 180, 360, and 540 s, respectively. The scale bars are 100 μm.

DOI:10.1063/1674-0068/28/cjcp1411201

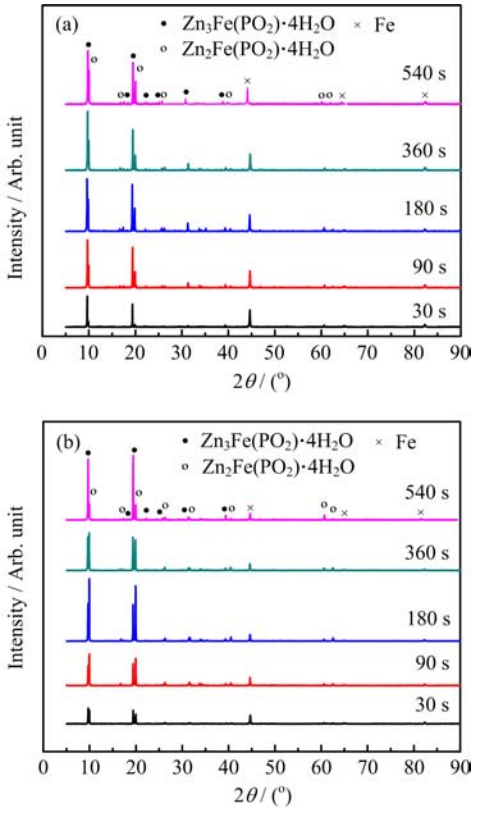

FIG. 5 XRD spectra of the phosphate coatings. (a) Treated by $NaNO_2$. (b) Treated by hydroxylamine sulfate.

grains gets smaller. Finally, the phosphate crystals continue to grow up until the end of phosphating reaction, as shown in Fig.4 (i) and (j).

XRD spectra of phosphate coatings are shown in Fig.5 when sodium nitrite and hydroxylamine sulfate are added into phosphate solution. It can be found that the main components of the phosphate coatings are $Zn_3Fe(PO_4)_2\cdot4H_2O$ (hopeite) and $Zn_2Fe(PO_4)_2\cdot4H_2O$ (phosphophyllite). With the increase of immersion time, the phosphate coating has become thicker and thicker. In Fig.5(a),the relative content of $Zn_3Fe(PO_4)_2\cdot4H_2O$ is higher than that of $Zn_2Fe(PO_4)_2\cdot4H_2O$ from the beginning to the end of the reaction, and from Fig.5(b) it can be seen that the relative content of $Zn_2Fe(PO_4)_2\cdot4H_2O$ is lower than that of $Zn_3Fe(PO_4)_2\cdot4H_2O$ from 30 s to 180 s.

C. Phosphate reaction mechanism

Now, it is widely recognized that the reactions which take place during phospahting process mainly include pickling reaction, coating reaction and sludge reaction. The first reaction (see reactions (1), (2), (3), and (4)), pickling reaction, is actually a chemical cleaning of metal surface, that is, metal ions are transferred into the phosphate solution. During this reaction, phosphoric acid is ionized and then hydrogen development is minimized owing to the presence of oxidation agents (accelerators such as $NaNO_2$). The second reaction is called coating reaction. During this process, pH rises and the metal cations cannot stay soluble in the solution because the free acid in the liquid-metal interface is continually consumed. The metal ions such as Zn^{2+} and Fe^{2+} react with the phosphoric acid radicals in the solution and then deposit on the metal surface as crystalline zinc phosphate. Depending on the process chemistry involved, several crystal structures such as $Zn_3Fe(PO_4)_2\cdot4H_2O$ (hopeite) and $Zn_2Fe(PO_4)_2\cdot4H_2O$ (phosphophyllite) are possible (see reactions (7) and (8)). The third reaction that occurs is so-called sludge reaction. During this process, sludge products are formed because Fe^{2+} in the solution is oxidized into Fe^{3+} ions and then react with the phosphoric acid radicals (see reaction (9)). Noticeably, zinc ions are incorporated in the coating reaction and no sludge is formed.

$$3Zn^{2+} + 2H_2PO_4^- \rightleftarrows Zn_3(PO_4)_2 + 4H^+ \quad (1)$$

$$H_3PO_4 \rightleftarrows 4H^+ + H_2PO_4^- \quad (2)$$

$$H_2PO_4^- \rightleftarrows H^+ + HPO_4^{2-} \quad (3)$$

$$Fe + 2H^+ \rightarrow Fe^{2+} + H_2\uparrow \quad (4)$$

$$NH_3OH^+ + 2H \rightarrow NH_4^+ + H_2O \quad (5)$$

$$4Fe + 10H^+ + NO_3^- \rightarrow 4Fe^{2+} + NH_4^+ + 3H_2O \quad (6)$$

$$Zn^{2+} + 2H_2PO_4^- + 4H_2O \rightarrow Zn_3(PO_4)_2\cdot4H_2O \quad (7)$$

$$2Zn^{2+} + Fe^{2+} + 2H_2PO_4^- + 4H_2O \rightarrow Zn_2Fe(PO_4)_2\cdot4H_2O \quad (8)$$

$$Fe^{2+} + 2H_2PO_4^- + NaNO_2 \rightarrow FePO_4\downarrow + NO\uparrow + NaH_2PO_4 + H_2O \quad (9)$$

$$3Fe + 2NO_2^- + 8H^+ \rightleftarrows 3Fe^{2+} + N_2\uparrow + 4H_2O \quad (10)$$

$$Fe^{2+} + NO_2^- + 2H^+ \rightleftarrows Fe^{3+} + NO\uparrow + H_2O \quad (11)$$

$$3Zn(H_2PO_4)_2 + 2Fe + 2NaNO_2 \rightleftarrows Zn_3(PO_4)_2 + 2FePO_4\downarrow + N_2\uparrow + 2NaH_2PO_4 + 4H_2O \quad (12)$$

As far as HAS is concerned, the NH_3OH^+ ions produced in the ionization process of HAS can react with hydrogen ions (reaction (5)) which are produced in reaction (2) and (3) and therefore the phosphating reaction (reaction (3)) is accelerated. When the concentrations of metal ions and phosphate radical ions reach the solubility product constant, the phosphate coating is formed with two types of crystals, *i.e.* $Zn_3Fe(PO_4)_2\cdot4H_2O$ and $Zn_2Fe(PO_4)_2\cdot4H_2O$ phases. Therefore, the effect of HAS is to some extent similar to the traditional nitrite and nitrate ions, whose reactions are given in (10), (11), and (12). However, as far as HAS is concerned, it is worth noting that no or trace amount of sludge is produced because no Fe^{3+} ions can be generated without the presence of oxidation agents. What is more, $NaNO_2$ has been widely recognized as a hazardous, noxious and carcinogenic substance. Consequently, wide popularization and application of HAS instead of $NaNO_2$ in phosphating industry is no doubt substantially important to

DOI:10.1063/1674-0068/28/cjcp1411201

the environmental protection. Correspondingly, it can be expected that HAS will be widely utilized as an efficient and ECO-friendly oxidant accelerator to replace nitrite (such as $NaNO_2$) although consumption of HAS is relatively higher than that of $NaNO_2$ in phosphating process.

D. Friction tests after surface saponification

The dependence of friction coefficient on time of samples after phosphating treatment and saponification is given in Fig.6. It can be found from Fig.6(a) that friction coefficient increases quickly at first (the first friction stage or initial friction stage) and then friction coefficient-time curve is turned to be smooth and steady (the friction coefficient ranges from 0.1 to 0.15). In fact, this stable friction stage (the second stage) can represent the real service lifetime of the lubricated samples. After 300 s, the friction coefficient starts to increase sharply (the third stage or severe friction stage), indicating that the saponification coating and phosphate coating are being worn off at a more rapid rate. At 400 s, the friction coefficient reaches its maximum, implying that most of the phosphate coating on the surface of the ball has been worn off. That is, the lubricated and phosphated sample has been in direct contact with the non-phosphated and non-saponified high carbon steel ball at this stage. In fact, it also implies the entire failure of the lubricated samples at this time. In contrast, the friction coefficient of samples treated by hydroxylamine sulfate (see Fig.6(b)) remains between 0.075 and 0.1 before 400 s, which is much lower than that of samples treated by $NaNO_2$. Consequently, it can be concluded that the samples treated by hydroxylamine sulfate instead of $NaNO_2$ have a better friction behavior.

Figure 7 shows the SEM surface morphologies of the above two samples after friction test. As shown in Fig.7, the substances in white areas, light areas and gray areas are referred as sodium stearate, substrate and the residual phosphate coating. Obviously, the content of residual phosphate coating treated by $NaNO_2$ is less than that of samples treated by hydroxylamine sulfate, which also implies that samples treated by hydroxylamine sulfate exhibit a better friction behavior compared with those treated by $NaNO_2$.

In addition, it can also be seen from Fig.4 that there are more dendritic phosphate crystals in phosphate coating treated by HAS than those in the coating treated by $NaNO_2$ (see Fig.4). Obviously, such relatively non-compact dendritic structure is to a great extent beneficial to the penetration of sodium stearate into the phosphate coating and the formation of zinc stearate with excellent anti-frictional capability. In sum, based on the above discussions, we believe that the samples treated by hydroxylamine sulfate instead of $NaNO_2$ have a better friction behavior and that the

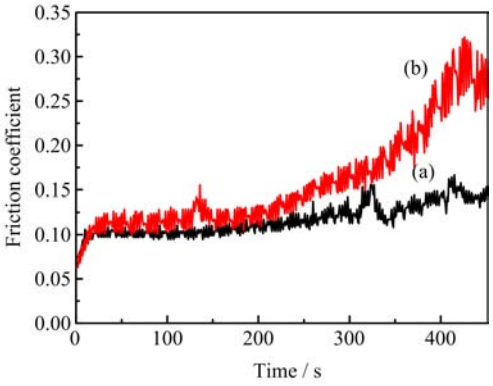

FIG. 6 Friction coefficient versus time. (a) Treated by $NaNO_2$ for 9 min. (b) Treated by hydroxylamine sulfate for 3 min.

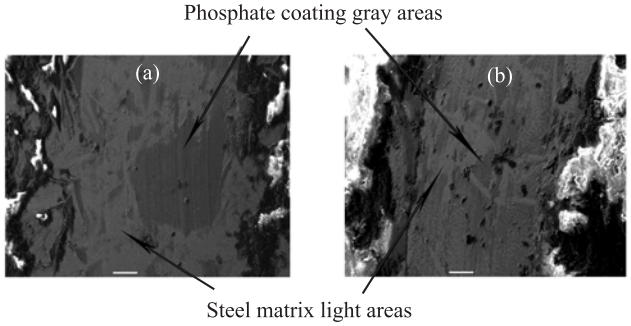

FIG. 7 SEM images of phosphate coatings after friction test (a) treated by hydroxylamine sulfate and (b) treated by $NaNO_2$. The scale bars are 1 μm.

phosphate solution with HAS will be widely applied in the plastic forming processes of steels such as wire drawing, cold heading and forging.

IV. CONCLUSION

In this work, hydroxylamine sulfate (HAS) and sodium nitrite were utilized to investigate their influences on the microstructure and frictional properties of zinc phosphate coating on high carbon steel substrate. Firstly, the phosphating parameters including temperature, time and the content of accelerators were optimized by utilizing orthogonal test method. Then, it is shown from XRD characterization that the coatings of samples treated by phosphate solution accelerated by HAS and $NaNO_2$ are mainly composed of hopeite $Zn_3Fe(PO_4)_2{\cdot}4H_2O$ crystals and phosphophyllite $Zn_2Fe(PO_4)_2{\cdot}4H_2O$ crystals with different shapes and sizes. In addition, the NH_3OH^+ ions from HAS can react with hydrogen ions and thus accelerates the phosphating reaction involved. Furthermore, no or trace amount of sludge is produced because no Fe^{3+} ions are generated in phosphate solution in comparison with $NaNO_2$. In summary, the samples treated by hydroxy-

DOI:10.1063/1674-0068/28/cjcp1411201

lamine sulfate instead of $NaNO_2$ have a better friction behavior, implying that HAS will be widely utilized as an efficient and ECO-friendly oxidant accelerator to replace nitrite (such as $NaNO_2$).

V. ACKNOWLEDGMENTS

This work was supported by the Bengbu Yucheng New Materials Science and Technology Ltd. (No.2012QTXM0375) and the Natural Science Foundation of Anhui Province (No.1208085QE99).

[1] V. Burokas, A. Martušinenė, and G. Bikulčius, Surf. Coat. Technol. **102**, 223 (1998).
[2] J. P. Bricout, P. Hivart, J. Oudin, and Y. Ravalard, J. Mater. Proc. Technol. **24**, 3 (1990).
[3] L. Gianfranco, Wire Ind. **61**, 385 (1994).
[4] M. Q. Sheng, Y. Wang, Q. D. Zhong, H. Y. Wu, Q. Y. Zhou, and H. Lin, Surf. Coat. Technol. **205**, 3445 (2011).
[5] A. S. Akhtar, K. C. Wong, and K. A. R. Mitchell, Appl. Surf. Sci. **253**, 493 (2006).
[6] M. Q. Sheng, Y. Y. Wei, and Q. D. Zhong, J. Coat. Technol. Res. **6**, 543 (2009).
[7] B. V. Jegdić, J. B. Bajat, J. P. Popić, S. I. Stevanović, and V. B. Miškovic-Stanković, Corros. Sci. **53**, 2872 (2011).
[8] J. M. Thomas and R. Rajia, Annu. Rev. Mater. Res. **35**, 315 (2005).
[9] V. R. Choudhary, P. Jana, and S. K. Bhargava, Catal. Commun. **8**, 811 (2007).
[10] F. Fang, J. H. Jiang, and C. Ma, J. Southeast Univ. Nat. Sci. Ed. **37**, 470 (2007).
[11] F. Fang, J. H. Jiang, S. Y. Tan, A. B. Ma, and J. Q. Jiang, Surf. Coat. Technol. **204**, 2381 (2010).
[12] M. C. M. Farias, C. A. L. Santos, Z. Panossian, and A. Sinatora, Wear **266**, 873 (2009).
[13] A. Kumar, S. K. Bhola, and J. D. Majumdar, Surf. Coat. Technol. **206**, 3693 (2012).
[14] L. Lazzarotto, C. Maréchal, L. Dubar, A. Dubois, and J. Oudin, Surf. Coat. Technol. **122**, 94 (1999).
[15] E. P. Banczek, P. R. P. Rodrigues, and I. Costa, Surf. Coat. Technol. **202**, 2008 (2008).
[16] S. Palraj, M. Selvaraj, and P. Jayakrishnan, Prog. Org. Coat. **54**, 5 (2005).
[17] N. Rezaee, M. M. Attar, and B. Ramezanzadeh, Surf. Coat. Technol. **236**, 361 (2013).
[18] L. Y. Niu, Z. H. Jiang, G. Y. Li, C. D. Gu, and J. S. Lian, Surf. Coat. Technol. **200**, 3021 (2006).
[19] A. S. Akhtar, D. Susac, P. Glaze, K. C. Wong, and K. A. R. Mitchell, Surf. Coat. Technol. **187**, 208 (2004).

DOI:10.1063/1674-0068/28/cjcp1411201